Landscape and Urban Planning 146 (2016) 29–42

Contents lists available at ScienceDirect

Landscape and Urban Planning

journal homepage: www.elsevier.com/locate/landurbplan

Research Paper

Hot playgrounds and children's health: A multiscale analysis of surface temperatures in Arizona, USA

Jennifer K. Vanos[a,*], Ariane Middel[b], Grant R. McKercher[a], Evan R. Kuras[c], Benjamin L. Ruddell[d]

[a] Atmospheric Sciences Research Group, Department of Geosciences, Texas Tech University, Lubbock, TX 79409-1053, USA
[b] School of Geographical Sciences and Urban Planning, Arizona State University, Tempe, AZ 85281, USA
[c] Department of Environmental Conservation, University of Massachusetts at Amherst, Amherst, MA 01002, USA
[d] Fulton Schools of Engineering, Arizona State University, Tempe, AZ 85281, USA

HIGHLIGHTS

- A mismatch exists between remotely sensed and *in situ* urban surface temperatures (T_s).
- The hottest T_s in a Phoenix area neighborhood were found on playground surfaces.
- Children are more vulnerable to the effects of heat stress and high T_s than adults.
- Shade of any type is found effective in reducing T_s and improving thermal safety.
- Data must be collected at the touch-scale for spatially accurate high T_s mitigation.

ARTICLE INFO

Article history:
Received 2 July 2015
Received in revised form 23 October 2015
Accepted 27 October 2015
Available online 10 November 2015

Keywords:
Surface temperature
Urban climate
Children's health
Playgrounds
Bioclimatic urban design
Geographic scale

ABSTRACT

Objectives: To provide novel quantification and advanced measurements of surface temperatures (T_s) in playgrounds, employing multiple scales of data, and provide insight into hot-hazard mitigation techniques and designs for improved environmental and public health.
Methods: We conduct an analysis of T_s in two Metro-Phoenix playgrounds at three scales: neighborhood (1 km resolution), microscale (6.8 m resolution), and touch-scale (1 cm resolution). Data were derived from two sources: airborne remote sensing (neighborhood and microscale) and *in situ* (playground site) infrared T_s (touch-scale). Metrics of surface-to-air temperature deltas (ΔT_{s-a}) and scale offsets (errors) are introduced.
Results: Select *in situ* T_s in direct sunlight are shown to approach or surpass values likely to result in burns to children at touch-scales much finer than T_s resolved by airborne remote sensing. Scale offsets based on neighbourhood and microscale ground observations are 3.8 °C and 7.3 °C less than the ΔT_{s-a} at the 1 cm touch-scale, respectively, and 6.6 °C and 10.1 °C lower than touch-scale playground equipment T_s, respectively. Hence, the coarser scales underestimate high T_s within playgrounds. Both natural (tree) and artificial (shade sail) shade types are associated with significant reductions in T_s.
Conclusions: A scale mismatch exists based on differing methods of urban T_s measurement. The sub-meter touch-scale is the spatial scale at which data must be collected and policies of urban landscape design and health must be executed in order to mitigate high T_s in high-contact environments such as playgrounds. Shade implementation is the most promising mitigation technique to reduce child burns, increase park usability, and mitigate urban heating.

1. Introduction

A neighborhood's thermal environment is complex. It is scale dependent and influenced by numerous physical characteristics such as weather, urban design, and the thermal properties of building and ground materials (Yaghoobian, Kleissl, & Krayenhoff, 2010). This complexity results in processes that impact health at several

* Corresponding author.
E-mail addresses: jennifer.vanos@ttu.edu (J.K. Vanos), amiddel@asu.edu (A. Middel), grant.mckercher@ttu.edu (G.R. McKercher), erkuras@gmail.com (E.R. Kuras), bruddell@asu.edu (B.L. Ruddell).

http://dx.doi.org/10.1016/j.landurbplan.2015.10.007
0169-2046/

scales, yet urban heat-health research often employs coarse scales collected from sparse standardized meteorological observations (BASC, 2012; Kuras, Hondula, & Brown-Saracino, 2015), which gives little evidence of linkages between urban form, air temperature, and surface temperature at the human scale.

Microscale urban climate models and remotely sensed data (on the order of 1 m^2 to 1 km^2) are often employed for heat stress analysis (e.g., Harlan, Declet-Barreto, Stefanov, & Petitti, 2013; Hondula et al., 2012; Masson, Champeaux, Chauvin, Meriguet, & Lacaze, 2003; Mishra, Ganguly, Nijssen, & Lettenmaier, 2015; Stefanov, Prashad, Eisinger, Brazel, & Harlan, 2004), with airborne remotely sensed data providing surface temperatures at a resolution ranging from 7 to 140 m (Stefanov et al., 2004). These scales may possess insufficient spatial resolution to determine certain personal health impacts based on micro-environmental heat exposure. The human-scale ranges from ~1.0 m for personal interactions with the proximate atmospheric and radiative microenvironment, to ~1 cm for touch-scale interactions. At this touch-scale, extreme temperatures can cause burns or damage to the skin, with a severity that depends greatly on the object's initial temperature, its material properties, and the contact thermal conductance (ISO 13732, 2010; Ungar & Stroud, 2010). In an outdoor urban environment, touch-scale surface temperature is based on urban design, material, orientation, and sun angle (e.g., Ketterer & Matzarakis, 2014a; Krayenhoff & Voogt, 2007). The touch-scale is on the order of 100× to 10,000× finer than that which remotely sensed data and urban climate models can currently provide. This variance therefore complicates spatially accurate design guidelines and policies.

The current study addresses the surface temperatures (ground and equipment) in small urban public playgrounds frequented by children aged 2–12 (ASTM F1487, 2011; CPSC, 2010). Urban parks, childcare play spaces, and urban playgrounds are important resources for urban sustainability, physical activity, and community health (Moore & Cosco, 2014; Vanos, 2015; Wolch et al., 2011). In the absence of design measures to mitigate heating, surfaces may become dangerously hot (e.g., Fig. 1), and playgrounds may become microscale heat islands that enhance, rather than mitigate, the larger urban heat island effect (UHI) (e.g., Moogk-Soulis, 2010). On clear, warm days with direct solar radiation, exposure to the mean radiant temperature (T_{mrt})—the combination of all short- and long-wave radiant fluxes (Thorsson, Honjo, Lindberg, Eliasson, & Lim, 2007)—becomes the most significant agent of heat gain to humans (Johansson, Thorsson, Emmanuel, & Krüger, 2014; Kántor & Unger, 2011; Mayer & Höppe, 1987), as well as to surfaces. The open design of urban parks with high radiant heat loads does not provide conducive spaces for safe physical activity and thermal comfort compared to shaded areas on warm–hot days (Koppe & Jendritzky, 2005; Matzarakis & Endler, 2010; Vanos, 2015; Vanos, Warland, Gillespie, Slater, et al., 2012). However, T_{mrt} can be reduced through design by (1) controlling incoming solar radiation with shade, indirectly reducing surface temperatures; and (2) by modifying surface materials to reduce surficial longwave radiation flux, indirectly reducing surface and air temperatures.

Quantifying temperature exposures (surface and air) in urban areas conserved for active use (i.e., parks and playgrounds) is important for understanding health effects (McGeehin & Mirabelli, 2001), and to adapt to future urban heating effects (Harlan & Ruddell, 2011; McCarthy & Sanderson, 2011), urban land use change (Adachi et al., 2013), and increasing temperatures with projected climate change (Meehl & Tebaldi, 2004; Tebaldi, Hayhoe, Arblaster, & Meehl, 2006). Most cities are not designed to ameliorate the effects of warming, although it is well known that this is possible through evidence-based climate-responsive design of urban spaces (Brown, Vanos, Kenny, & Lenzholzer, 2015; Erell, Pearlmutter, & Williamson, 2012; Masson et al., 2014; Middel, Chhetri, & Quay, 2015). Properly designed playgrounds contribute to microscale cooling, serving as heat refuges through the summer season (Cheng, Wei, Chen, Li, & Song, 2014; Chow, Pope, Martin, & Brazel, 2011; Vanos, Warland, Gillespie, Slater, et al., 2012), as well as comfortable and safe places for children to play and engage in activities for improved health and well-being (Ciucci et al., 2013; Moore & Cosco, 2014; Vanos, 2015; Wolch et al., 2011).

Children are uniquely sensitive and vulnerable to hot ambient environments as compared to adults (Balbus & Malina, 2009), mainly due to their high ratios of both metabolism-to-surface area, and surface-area-to-body-mass (Falk & Dotan, 2008; Wenger, 2003), resulting in thermoregulatory inferiority relative to adults during physical activity in hot conditions (Falk & Dotan, 2008). Such hot conditions result in air temperature becoming greater than skin temperature, and convective heat (which is normally a loss of heat from the skin's surface) becomes a gain and thus a quicker path to heat stress for children. In the same sense,

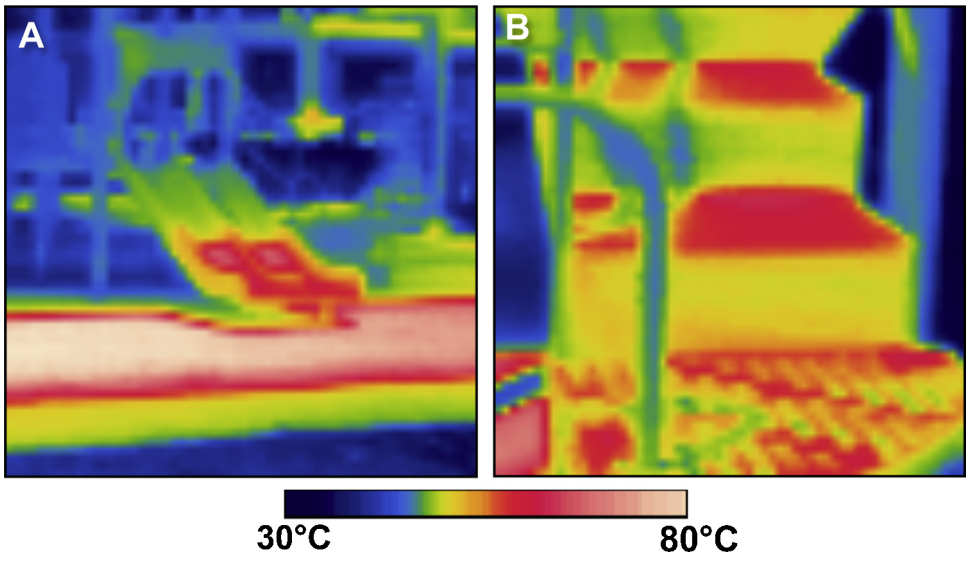

Fig. 1. Surface temperature images photographed in the study playgrounds using Infrared Thermography (IRT) (FLIR camera, TG165). (A) Slide and black/green rubber ground surface in sun (71 °C on slide; 82 °C on rubber), and under shade sail (blue/green); (B) playground steps in sun, black powder-coated metal (58 °C). Photos were taken at 1045 h LST. (For interpretation of the references to color in this figure legend, the reader is referred to the web version of this article.)

Table 1
Burn thresholds when skin is in contact for short periods of time (3 s, 5 s, 1 min) with hot surfaces made of materials commonly found within playgrounds. Thresholds of materials with similar heat conductivity are combined to represent one value.

Material	Material characteristics	Burn threshold (°C)		
	Contact time	3 s	5 s	1 min
Metal	Uncoated	60 °C	57 °C	51 °C
Coated metal[a]	Lacquer coat: 100 μm	68 °C	61 °C	51 °C
	Powder: 90 μm	65 °C	60 °C	51 °C
	Enamel: 160 μm	63 °C	59 °C	51 °C
	Polyamid 11 or 12: 400 μm	77 °C	70 °C	51 °C
Stone material	Concrete, granite, asphalt	73 °C	60 °C	56 °C
Plastic[b]	Polyamide, acrylglass, polytetrafluorethylene, duroplastic	77 °C	74 °C	60 °C
Wood	Bare, low moisture	99 °C	93 °C	60 °C

Source: ISO 13732 (2010).
[a] Polyurethane enamel-coated steel is used predominantly in the study site playgrounds for hold/touch surfaces, and powder coated steel for walking surfaces.
[b] UV stabilized high-density polyethylene (HDPE) used in playgrounds is similar in material properties to polyamide.

children will cool off more quickly if a cooler space is provided, such as a shaded area. Children's sweating rates are also lower than that of adults, thus they rely mainly on dry heat dissipation through convection (Falk & Dotan, 2008), which is not effective in extreme heat. Lastly, children are more susceptible to burn injuries on playground equipment due to more sensitive skin (Oliveria, Saraiya, Geller, Heneghan, & Jorgensen, 2006), slower reflexes to remove their hand from what may be causing the burn (ISO 13732, 2010), and the lack of experience in the causes and effect of burns (Ford, Moriarty, Riches, & Walker, 2011). This lack of experience results in differences in the perception of heat between children and adults, where expectations and experience, perception, personal preference, and feedback mechanisms related to the thermal environment (e.g., Knez, Thorsson, Eliasson, & Lindberg, 2009; Metje, Sterling, & Baker, 2008; Parsons, 2003) are more limited in children, affecting the interpretation of their physical state and subsequent adaptive behavior to avoid heat stress (Vanos, 2015).

Due to many of the above-mentioned cumulative factors, children experience burns on playgrounds even in moderate mid-latitude climates (Ford et al., 2011; Strong, Tahir, & Verma, 2007). Burns can occur in 3 s on solid metal surfaces with temperatures ≥60 °C (ASTM 1055, 2014; CPSC, 2010; ISO 13732, 2010; Ungar & Stroud, 2010); for plastics or nonmetallic coatings that are more insulating, higher threshold temperatures are set (e.g., ≥77 °C for plastic ISO 13732 (2010), see Table 1). Guidelines in the United States for public playground safety are put forth by the U.S. Consumer Product Safety Commission (CPSC) (CPSC, 2010) and contain suggestions and information for the use of materials and coatings, as well as the orientation of objects with respect to sun angles; however, *in situ* quantitative evidence is lacking to adequately guide designers on the implementation and material of equipment based on bioclimatic design principles. Although the guidelines are set by the CPSC to minimize injury to children, a small number of burns continue to be reported, e.g., 14 severe burns in American playgrounds reported between 2001 and 2008 (Ford et al., 2011; O'Brien, 2009).

Accordingly, the goal of this study is to provide novel quantitative insight into the multiscale issues of the thermal microenvironment in two playgrounds in Gilbert, Arizona. We focus on touch-scale surface temperature variations in comparison with remotely sensed surface temperatures (6.8 m resolution) and the real-world applicability of such data based on scale. The role of shade (natural and artificial) in altering surface temperatures to mitigate burn risk is also quantified at the touch-scale. We address how overlooking sub-grid scale variation in airborne remotely sensed surface temperatures in playgrounds may result in inferior evidence for planning, decision-making, and the establishment of equipment safety standards related to playground burns and heat stress in children.

2. Methods

2.1. Study site

Within the Master Planned community of Power Ranch (33.27040, −111.69527) in Gilbert, Arizona, USA, two playgrounds (denoted as the North and South Playground) comprised the *in situ* sites in the current study (Fig. 2). This community is in the southeast valley of metropolitan Phoenix, just on the edge of Phoenix's large UHI effect (Chow, Brennan, & Brazel, 2012). Phoenix is the U.S. metropolitan area with the highest summer temperatures (National Oceanic and Atmospheric Administration, 2012), averaging 74 days per year with daily maximum air temperatures at or above 40 °C. These high temperatures are shown to be associated with the highest risk for heat-related morbidity (Petitti, Hondula, Yang, Harlan, & Chowell, 2015), which can be particularly dangerous for the most socially vulnerable, low income, and isolated populations (Harlan et al., 2013). Moreover, the desert Southwest is warming faster than most US regions and is projected to warm at a high rate in the coming decades (Karl, Melillo, & Peterson, 2009; Walsh et al., 2014), with the temperature change in the hottest days projected to increase by approximately 5.5–8.5 °C under a high emissions scenario (Luber et al., 2014).

The Power Ranch community features parks, playgrounds, walking trails, ponds, splash pads, swimming pools, athletic fields, and meeting spaces. A dozen adjacent neighborhoods comprise Power Ranch, each organized around a central park (which contains the North Playground) where residents walk dogs, exercise, and congregate. Two elementary schools within the community host over 1400 students combined (HUSD, 2015a,b). 13.2% of the residential population is less than 5 years of age and 27.9% is between the ages of 5 and 17. The median age of Power Ranch residents is 27.4 years and the median household income is $75,642 (U.S. Census Bureau). The community is predominantly white (91.0%), with 4.2% Black or African American ethnicity, 4.7% Asian, 20.6% Hispanic or Latino, and 2.9% identifying as 'other'.

The locations of the two playgrounds are displayed in Fig. 2, with examples of the playgrounds and equipment provided in the Supplemental material. Each playground contains numerous pieces of common playground equipment and 2–3 benches. The North playground spans a rectangular area of 497 m^2, and its surface cover is predominantly sand and concrete, with some black/green soft rubber. A swimming pool and basketball court are nearby. The NASA MODIS/ASTER Airborne Simulator (MASTER, Hook, Myers, Thome, Fitzgerald, & Kahle, 2001) overflight took place on July 13, 2011 between 1100 and 1330 h, collecting land surface temperatures (LST) at a resolution of 6.8 m (see Section 2.2.1 for MASTER details). On this date, there was no shade sail present in the North playground; however, in 2013 when the *in situ* data collection took place, a large shade sail (12 m × 17 m) was installed in the North

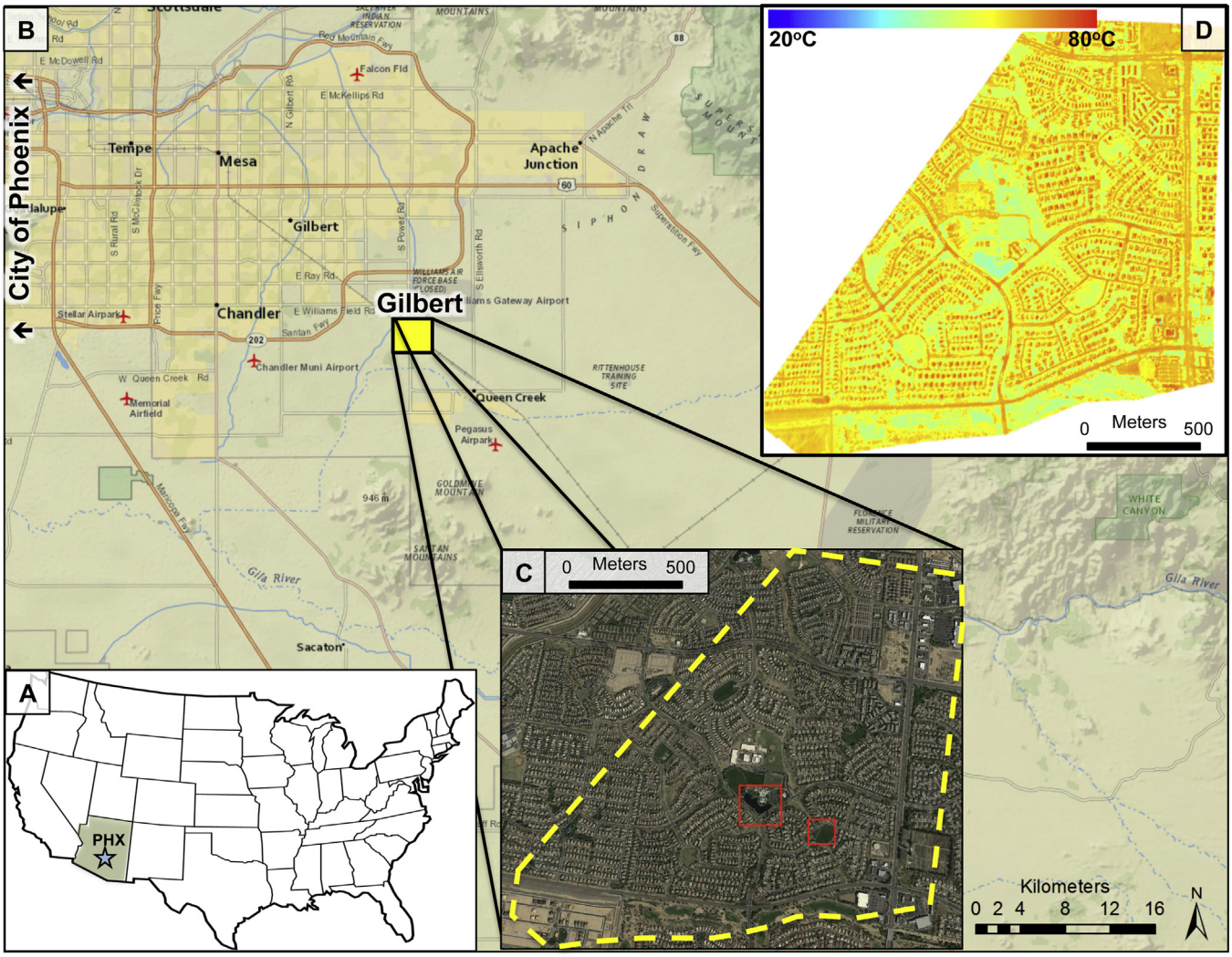

Fig. 2. (A) Location of the state of Arizona (green shading) in the USA, and the Phoenix Metropolitan Area (PMA) (star with PHX label); (B) map of east PMA (with the city center to the west), identifying the location of the study site of Gilbert containing the Power Ranch Neighborhood in yellow; (C) Visible overhead image of the Power Ranch neighborhood with playground location in red boxes; (D) Thermal Infrared MASTER super spectral image of Power Ranch neighborhood obtained midday (1100–1330 h) on July 13, 2011.

playground. The addition of the shade sail between the two study years provides a unique opportunity for a natural experiment to assess the improvement in the thermal environment created by the investment in the sail. Surfaces that are adequately shaded will generally demonstrate little-to-no difference from air temperature during the daytime. Within the 497 m^2 rectangular area of the North playground, no trees are present, however three ash trees to the southwest of the area provide shade in the late afternoon hours. The common tree types found within the 25 m radius from the center of the North playground are the southwestern urban tree species of Shamel Ash, Palo Verde, Western Cedar, Willow Acacia, and Mesquite. Hence, in the area outside of the playground area, tree canopy provides some shade, however minimal to the playground itself.

The South playground is circular, 402 m^2 in area, with sand as the playing surface. A basketball court is nearby, and there is no shade sail present. Within the circular playground itself, two Cottonwood trees are found with canopy covering ~5% of the play area. The common tree types found within the 25 m radius of the playground's center include Southern Live Oak, Western Cedar, Cottonwood, and Shamel Ash. The two Cedar trees and the Cottonwood tree to the south and southwest of the playground provide shade in the late afternoon hours. For both parks, the trees are approximately 15–20 years of age, with a mature height, are well-maintained, and in good health. Finally, trees were in full leaf with average shading coefficients ranging from 0.65 (Mesquite) to 0.85 (Cottonwood, Palo Verde).

2.2. Data acquisition

2.2.1. Airborne data

Superspectral data acquired by the NASA MODIS/ASTER Airborne Simulator (MASTER) (Hook et al., 2001) were used to investigate LST for the full Power Ranch neighborhood, including the two playground study sites. MASTER is an aircraft mounted multispectral sensor system that provides the same observations as NASA's MODIS and ASTER satellites, but at higher resolution owing to the much lower altitude of airborne observations (e.g., 6.8 m resolution for the Thermal Infrared (TIR) product) (Hook et al., 2001). This TIR data captures near-peak surface temperatures (T_s) with a higher spatial and spectral resolution compared to many sensor systems (e.g., Stefanov et al., 2004; Van Der Meer & de Jong, 2001). The MASTER data used in this study were acquired midday (1100–1330 h LST) on July 13, 2011 (Jenerette et al., 2015). The geo-referenced LST data are further extracted by each parcel polygon (obtained from cadastral GIS vector layer) to represent the

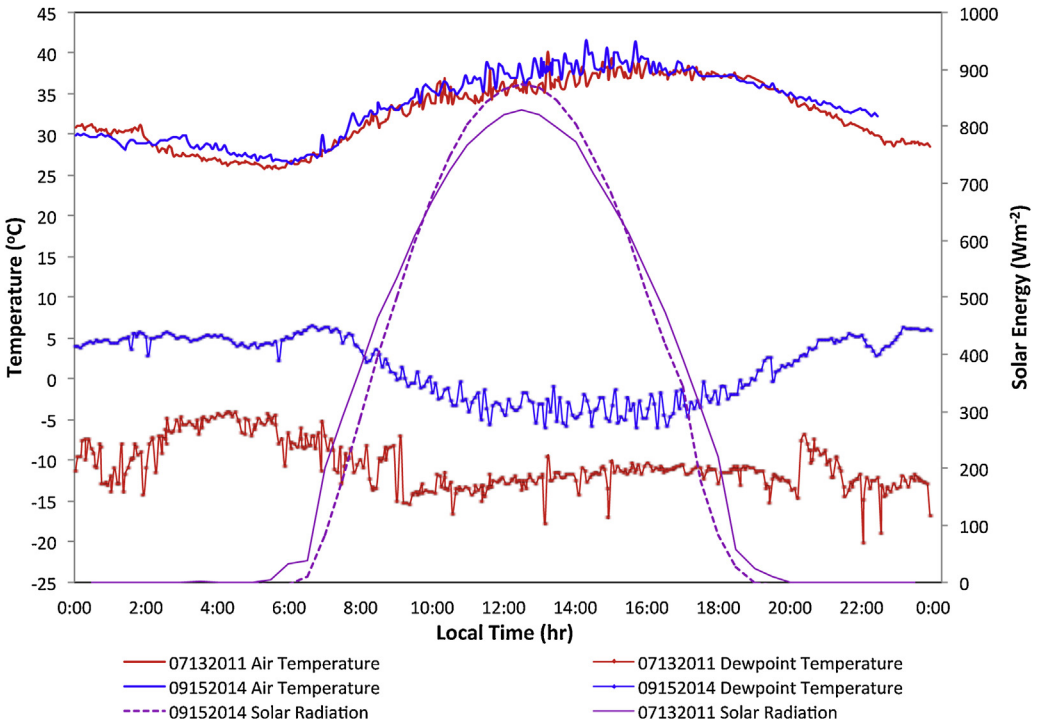

Fig. 3. Diurnal variations in air temperature, dew point temperature, and solar radiation for the two dates of comparisons (July 13, 2011 and September 15, 2014).

parcel mean LST (see Fig. 2). Further details regarding the MASTER overflight and processing of the data to obtain LST can be found in Jenerette et al. (2015). The retrieved resolution (6.8 m) of the T_s data from the MASTER sensor allow for microclimate-related analysis and also allow for comparison with touch-scale *in situ* site playground measurements detailed below.

2.2.2. Playground site data

On September 15, 2014, *in situ* ground-based microclimate data were collected within each playground from 1200 h to 1400 h LST using research-grade instruments obtained from Campbell Scientific (Logan, Utah). Air temperature (T_a) was measured using high accuracy fine-wire chrome–constantan (Type 'E') thermocouples at 1 m and 2 m height. A secondary measurement of T_a and relative humidity was taken using an HC-S3 sensor probe at 1 m and 2 m height. T_a collected at a 2 m height was used for analyses. Total incoming solar radiation was measured using an SC300 silicon photovoltaic pyranometer. All above-listed instruments were securely mounted on a mobile golf cart. For September 2011, air and dew point temperatures and solar radiation were collected using a scientific grade WeatherHawk signature meteorological station, 3 m height over grass, located approximately 100 m from the center of Power Ranch with comparable measurements calibrated to the same standard as the mobile station. This was used for comparative purposes with the *in situ* field day collected at 2 m over grass on September 2014, as displayed in Fig. 3.

Two types of *in situ* infrared thermometry (IRT) T_s measurements were made: (1) hand IRT measurements taken at 1 cm perpendicular to the surface of interest using a DeltaTrak ThermoTrace Handheld infrared thermometer (Pleasanton, CA); (2) cart-mounted measurements (front of cart mounted 30 cm from surface) with SI-111 Precision Infrared Radiometers (Campbell Scientific, Logan, Utah). Emissivity corrections were made for surfaces with low emissivity, as the IRTs assume an emissivity equal to 0.95. Surface temperature images were also taken using Infrared Thermography (FLIR camera, TG165) (e.g., Fig. 1).

Selection of surfaces for hand IRT was based on an intersection of the following two criteria: (1) objects presenting high quality sampling opportunities featuring both full direct perpendicular sun angle and full shade; (2) objects that had a high likelihood to be walked on, sat on, or held for ≥3 s (such as the ground, steps, slides, benches, handrails, and seats). Full shade and direct perpendicular sun exposure were chosen to represent the extreme bounding conditions inclusive of all types of solar angles and partial shading. Surface solar exposure was of three classes: full direct perpendicular sun, natural shade (i.e., tree), and artificial shade (e.g., shade sail, pavilion, building shadow).

2.2.3. Multiscale metrics and temporal analyses

In order to standardize the T_s for comparative purposes between scales, we calculate the relationship of the difference ('*delta*') between the surface temperature and 2 m air temperature (T_s). This delta method allows for a relatively unbiased comparison of the T_a between the three scales of measurement (touch-, micro-, and neighborhood scales) using the T_a values that are in approximate equilibrium with respect to time and sun/shade. This is in contrast to using only the magnitude of T_s between two differing surfaces in sun and/or shade that do not have standard T_s values at the different scales for comparison. This is particularly important for the playground equipment, where the touch-scale deltas between T_a and T_s are hypothesized to increase as we approach maximum T_a (mid-afternoon). However, this delta is expected to be lesser at the 1 km scale (neighborhood) at mid-afternoon, where due to the coarse-scale averaging, the measurements of T_s will be closer to that of T_a (hence, $T_{a\_1\mathrm{km}} \cong T_{s\_1\mathrm{km}}$).

A second metric is also employed to compare deltas by scale, denoted as the '*scale offset*'. The scale offset represents the difference of the $\Delta\bar{T}_{s-a}$ between scales. We first assess the mean differences within the scale making use of the delta method above ($\Delta\bar{T}_{s-a}$), and secondly we calculate the differences in the delta between scales, which gives the scale offset (representing an error). This offset provides dual benefits for interpretation of results in the current study as it relates both $\Delta\bar{T}_{s-a}$ and $\bar{T}_s$ at the different scales of observations, thus demonstrating how spatial uncertainty is influenced by the context of measurement.

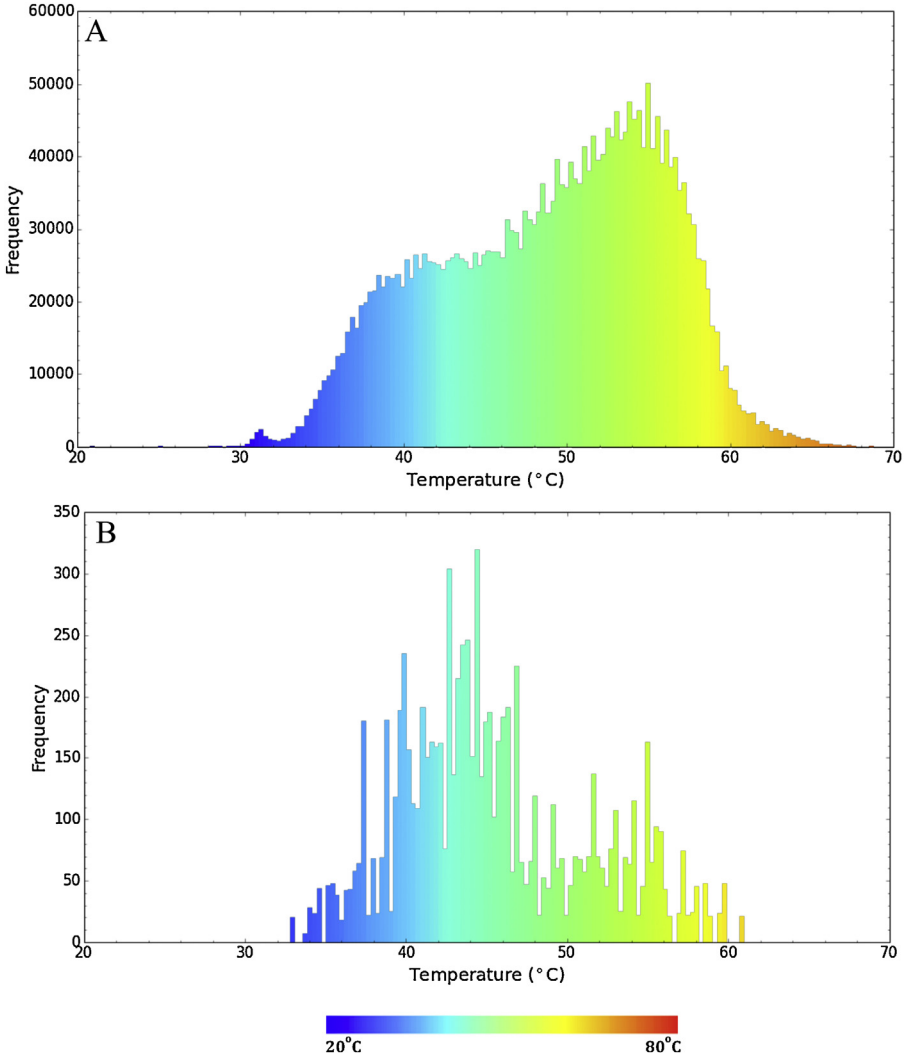

Fig. 4. Frequency histograms of surface temperatures in (A) Full Power Ranch neighborhood, including parks and playgrounds, and (B) study site playgrounds and their immediate surroundings within the Power Ranch neighborhood.

Further interpretation employs the sky view factor (SVF) for each location where a touch-scale T_s measurement was taken. Fisheye photos of the sky were taken at each observational stop at a height of 1.5 m. The SVFs were calculated from these photos using Rayman 2.1 (Matzarakis, Rutz, & Mayer, 2010). All hand IRT readings were completed in less than 10 min in the time periods surrounding 1230 h LST; however, the cart-mounted T_s were obtained in a neighborhood transect during a 2 h sampling period. To account for the warming of the air and surfaces that takes place during each transect, observations were normalized to a fixed point in time (time detrended), assuming a linear increase in T_s over the 2 h period. An empirical warming rate was calculated using a linear regression based on the observations. Using the regression equation, observations were normalized to 1230 h LST for comparison to playground hand IRT readings.

Although time detrending has the benefit of making the data points comparable across time, comparing derived measurements (e.g., $\Delta\bar{T}_{s-a}$ and scale offsets) using a time detrending function that is based on all samples is unfavorable as different surface types have different heating/cooling rates in the sun/shade. For example, if a heating rate for sun-exposed asphalt is applied to shaded grass, then the function will overestimate the heating correction for grass T_s. During sampling in the current study, all sun-exposed surfaces were collected within the first 15 min of analysis, thus heating was minimal. Therefore, this is merely an issue with shaded surfaces that were sampled 30–60 min later. However, the sun-exposed surfaces heat at a much faster rate introducing bias if using the all sample ('global') regression function for shaded surfaces (i.e., the regression over-corrects for heating that took place on sun exposed surfaces but not on shaded surfaces). As this error produced by the regression function increases over time, we employed the T_s data in their original state, even with slight heat/cooling variability, and accept a slight warming of the shaded surfaces (1 °C for grass and 2 °C for concrete over the transect period) that may not be comparable across time. This error is only present in the tree analysis and does not affect the playground surface T_s. In order to calculate an average-rate correction factor for the time detrending for each surface type and each exposure separately, further *in situ* data are required, which will build upon the foundation provided by the current study.

3. Results

3.1. Daily microclimate variations

Fig. 3 displays the daily patterns of air and dew point temperature, and incoming solar radiation on July 13, 2011 and Sept 15, 2014. Both days were classified as 'Dry Tropical' weather

Table 2
In situ surface temperature measurements taken at site playgrounds, September 15, 2014. Temperatures measured (1200–1300 h LST). Corresponding materials, thermal conductivities, and average albedos for each surface also listed (ASTM C1057, 2012; Campbell & Norman, 1998; Environmental Protection Agency, 2014; ISO 13732, 2010; Oke, 1988; Paul, Pal, Ghosh, & Chakraborty, 2004).

Equipment	Thermal cond ($W m^{-1} K^{-1}$)	Albedo mean (range)	Playground surface temperatures		
			T_s (°C) Sun	T_s (°C) Shade (tree)	T_s (°C) Shade (sail)
Seating use children					
Slide[a] (beige)	0.25–0.51	0.18 (0.15–0.20)	63.9	40.6	–
Bouncy spring rider[a] seat (green)	0.25–0.51	0.18 (0.15–0.20)	55.0	44.4	–
Bouncy spring rider[a] seat (red)	0.25–0.51	0.18 (0.15–0.20)	57.2	45.0	–
Bouncy spring rider[a] seat (yell/blue)	0.25–0.51	0.18 (0.15–0.20)	46.7	–	37.8
Slide[a] (green)	0.25–0.51	0.18 (0.15–0.20)	71.7	43.9	–
Walking use (foot contact)					
Asphalt	0.75	0.13 (0.05–0.20)	53.7–60.7	32.9–40.2	–
Sand	0.15–0.25	0.33 (0.25–0.40)	59.4–62.8	32.8–33.9	33.9–35.3
Steps and Walkway[b] (black)	45.20	0.08 (0.02–0.14)	60.0	39.4	41.1
Basketball surface asphalt (green paint)	0.75	0.28 (0.05–0.50)	60.0	–	–
Basketball surface asphalt (white paint)	0.75	0.38 (0.25–0.50)	51.7	–	–
Rubber soft ground surface (blk/green)	0.29	0.10 (0.05–0.15)	87.2	42.2	46.7
Splash pad[c] (white/blue)	0.29–0.62	0.38 (0.30–0.45)	42.2	27.8	–
Concrete	1.00–2.50	0.38 (0.30–0.45)	49.5–56.0	31.8–40.5	35.2
Grass	1.10	0.25	38.1–40.1	30.6–43.2	–
Pool deck[d] (light gray)	1.00–1.80	0.38 (0.30–0.45)	52.2	–	–
Crushed granite	0.20–0.90	0.57 (0.14–1.00)	54.2	35.0–42.2	–
Holding (hand contact)					
Balance rail (red)[e]	0.22	0.20 (0.10–0.30)	62.2	–	–
Bouncy spring rider handle[e] (green)	0.22	0.20 (0.10–0.30)	55.0	–	–
Bouncy spring rider handle[e] (red)	0.22	0.20 (0.10–0.30)	43.9	–	–
Posts of playground structure[e] (purple)	0.22	0.20 (0.10–0.30)	51.1	38.3	38.9
Posts of playground structure[e] (green)	0.22	0.20 (0.10–0.30)	51.7	–	–
Boardwalk railing[a] (brown)	0.22	0.20 (0.10–0.30)	68.3	–	–
Railing[e] (blue)	0.22	0.20 (0.10–0.30)	48.9	40.0	–
Railing[e] (brown)	0.22	0.20 (0.10–0.30)	61.1	–	–
Railing[e] (red)	0.22	0.20 (0.10–0.30)	55.0	–	–
Railing[e] (green)	0.22	0.20 (0.10–0.30)	–	40.0	42.2
Post of shade structure[e] (beige)	0.22	0.20 (0.10–0.30)	46.7	–	37.8
Steering wheel[e] (brown)	0.22	0.20 (0.10–0.30)	48.3	39.4	–
Basketball post[b] (gray)	45.20	0.08 (0.02–0.14)	47.8	–	–
Parent or child seating					
Bench (metal, rubber coated)	0.22	0.20 (0.10–0.30)	50.0	40.0	–
Bench[a]	0.42–0.51	0.18 (0.15–0.20)	63.9	–	–
Miniature stools[a] (brown)	0.25–0.51	0.18 (0.15–0.20)	48.3	–	–

[a] Molded plastic (UV stabilized high density polyethylene (HDPE)).
[b] Powder-coated steel.
[c] Rubber pad, slightly moist.
[d] Light colored, textured, slip-resistant concrete.
[e] Polyurethane enamel-coated steel.

types (Sheridan, 2002, 2015) with clear skies. There was little difference in the T_a between the two days, with means (ranges) of 32.6 °C (25.8–40.2 °C) and 33.6 °C (26.4–41.6 °C), respectively. Hence, the maximum 2 m T_a was 40.2 °C on July 13, 2011 and 41.6 °C on September 15, 2014. This ~1 °C average difference is insignificant, and minor given that it is the rough estimate of error assumed in the mean temperature delta ($\Delta\bar{T}_{s-a}$) caused by meteorology on the given day. The average daily incoming solar radiation was 502 $W m^{-2}$ on July 13, 2011 and 519 $W m^{-2}$ on Sept 14, 2014, with maximum radiation intensities reaching 829 $W m^{-2}$ and 874 $W m^{-2}$ at 1230 h LST for both days, respectively.

3.2. Surface temperature variation

This study quantifies the T_s and ΔT_{s-a} of two neighborhood playgrounds at three spatial scales of measurement: 1 km neighborhood scale, 6.8 m microscale, and 1 cm touch-scale. We present results at the microscale, followed by a touch-scale analysis, and finally an integration of the datasets that address the distributions of T_s at each scale incorporating the *delta* and *scale offset* temperatures.

3.2.1. Remote sensing data: 6.8 m scale

The TIR-based T_s product from the MASTER airborne data allows for T_s estimation of objects at a resolution of 6.8 m or greater, such as roads, buildings, houses, backyards, street medians, swimming pools, and basketball courts. A total of 2,731,883 pixels representing T_s were obtained from the MASTER airborne data for the Power Ranch neighborhood between 1100 h and 1330 h LST on July 13, 2011. The average 6.8 m pixel T_s within the entirety of the neighborhood was 48.8 °C (SD = 6.89 °C), ranging from 15.8 °C (representing water) to 71.4 °C (dark asphalt and roofs). Data from both playgrounds were combined to form a subset of the full neighborhood data. The playground 6.8 m T_s was 45.3 °C (SD = 5.89 °C), ranging from 32.8 °C (moist pool deck) to 60.7 °C (sand, asphalt).

The distributions of these temperatures (full neighborhood and a subset of the two playgrounds combined) are displayed in Fig. 4. The probability distribution of the full neighborhood is skewed to the right (skew = −0.45) signifying the bulk of the temperatures greater than the median, while the playground distribution is skewed to the left (skew = +0.52). The most common 6.8 m T_s (the mode) is 54.9 °C in the neighborhood (which is above the neighborhood mean), and 44.3 °C in the playgrounds (which is below the playground mean). This 6.8 m resolution misses human scale and

touch-scale details that are important for thermal health, such as sun versus shade, that were observed in the 1 cm T_s data collected at touch-scales with the IR thermometers. This 6.8 m MASTER product is also not able to 'see' surface temperatures under shade structures or trees and misses the shade effects entirely, yielding tree canopy and roof top temperatures rather than the actual surface temperatures that are experienced by neighborhood residents.

3.2.2. In situ*: 1 cm touch scale*

The range of the 1 cm touch-scale T_s is compared across objects grouped into three categories of use: 'sitting', 'walking', and 'holding', as listed in Table 2. Wide ranges in the T_s are present between various playground features and ground cover in both open sun and shade (natural and artificial). The maximum 1 cm touch-scale T_s was 87.2 °C, measured on the soft rubber ground (black/green in color) installed in place of a natural ground surface. In the shade, this rubber surface's T_s decreases to 42.2 °C (tree shade) and 46.7 °C (shade sail), representing a ΔT_s of 45.0 °C and 40.5 °C, respectively. Playground walking surfaces bore an average T_s of 56.0 °C in the sun, 36.9 °C in the shade of trees, and 39.3 °C under a shade sail. This yields a mean ΔT_s of −19.1 °C in tree shade, and −16.7 °C for artificial shade by the shade sail. Five of the ground surfaces measured with hand IRT (rubber surface, sand, steps, walkway, and the basketball courts) surpass their material specific threshold for burn based on a 5 s contact time (Table 1); however, natural or artificial shade brings these five surfaces to safe values for touch.

The 1 cm scale T_s of playground equipment sat on by children range from 46.7 °C to 71.7 °C in the sun. The plastic bench intended for seating (T_s = 63.9 °C) surpasses the 1 min 60 °C threshold for plastic, while slide temperatures also presented high T_s values of 71.7 °C and 63.9 °C for the green and beige slides, respectively (e.g., see Fig. 1). However, under shade trees the T_s of these sitting surfaces decrease by 18.5 °C on average, and thus are brought into a safe range for sitting. Lastly, for objects that are held by children, the T_s ranges from 43.9 °C (spring rider handle) to 68.3 °C (boardwalk railing). The majority of these "holding" objects were present in full sun, which resulted in few sun versus shade comparisons of T_s on the given holding objects; however, playground structure posts were commonly found in both sun and shade, with T_s decreasing by an average of 11.3 °C in the shade.

3.2.3. Surface-to-air temperature variations by scale

It is evidenced above that shade has the ability to substantially reduce the T_s of both artificial and natural surfaces by intercepting shortwave radiation. The SVF (inverse of the species shading coefficient) is used here as a general interpretive framework for all types of shade, including shade sails and artificial shade. In addition, in order to standardize the T_s for comparative purposes, the ΔT_{s-a} is employed and further interpreted using the SVF (Fig. 5). Surfaces that are adequately shaded (low SVF) generally demonstrate no difference from T_a during early afternoon, while those with high SVFs have a high proportion of the surface exposed, thus an increased T_s is found. This is a new type of multiscale model for ΔT_{s-a} as a function of surface type and SVF, and in this implementation the model can be used to relate 6.8 m remotely sensed T_s to touch-scale and (partially) shaded T_s in early afternoon. The same principles apply to other times of day, seasons, and locations, but the model's coefficients need to be estimated separately for those applications.

Within Fig. 5, we further see that the ΔT_{s-a} values increase with SVF, with a combined moderate Pearson's correlation of r = 0.64. Linear regressions are presented to show the positive relationships of ΔT_{s-a} over each surface type with SVF; however these are not statistically significant due to low sample numbers, and are presented for visual purposes only. The $\Delta \bar{T}_{s-a}$ values also vary by surface type in both sun and shade (Table 3), with natural grass demonstrating the smallest delta when shaded ($\Delta \bar{T}_{s-a}$ = −5.5 °C), thus resulting in T_s much lower than T_a. This $\Delta \bar{T}_{s-a}$ is 3.7 °C cooler than the average delta in the shade for all surfaces combined ($\Delta \bar{T}_{s-a}$ = −1.8 °C). It is important to note here that irrigation practices and practitioners are consistent between the study periods. The Power Ranch Community Association's landscapers use a computer-controlled irrigation system that waters the grass every night, and trees every several days, during the summer season. Root zone soil moisture is kept above deficit levels, and by early afternoon any residual surface moisture has evaporated. This should result in nearly constant evapotranspiration rates and T_s during afternoon hours between the two study periods.

Table 3
Mean differences between surface and air temperatures ($\Delta \bar{T}_{s-a}$) in open sun or tree shade cover based on surface type within playgrounds.

	$\Delta \bar{T}_{s-a}$ (°C) 1 cm scale	
	Shade	Sun
Asphalt	0.1	22.3
Concrete	−0.7	14.7
Grass	−5.5	3.5
Rock	−1.3	16.7
Sand	−1.6	23.0
Average	−1.81	16.04

Table 4
Offset values representing the difference in the mean surface-to-air temperature deltas ($\Delta \bar{T}_{s-a}$) in the playground of (A) the 1 cm touch-scale deltas versus 6.8 m sand deltas, and (B) the 1 cm touch scale delta versus the 1 km delta. Offsets represent potential T_s errors when using the 6.8 m and 1 km scales, respectively, for playground equipment analysis.

Burn threshold (°C)	(A) Playground offset of 1 cm to 6.8 m scale (°C)	(B) Playground offset of 1 cm to 1 km scale (°C)
Sitting – child	13.6	10.1
Walking	9.9	6.4
Holding	8.0	4.5
Sitting – adult and child	8.8	5.3
Average	10.1	6.6

Shaded asphalt demonstrates the least deviation from T_a ($\Delta \bar{T}_{s-a}$ = 0.1 °C). In the open sun, the asphalt and sand result in the greatest deviation from T_a (22.3 and 23.0 °C, respectively), much higher than the average for all surfaces in the sun combined ($\Delta \bar{T}_{s-a}$ = 16.0 °C). These stark contrasts in surface-to-air temperature differences based on surface type and SVF highlight the importance of surface type when modeling the effect of sun and shade on T_s. We also find that the type of tree providing shade does not result in significantly different surface-to-air temperature deltas, demonstrating that the SVF has little variation between the tree specifies in the neighborhoods during the summertime, and that each tree provided enough shade to provide a large T_s reduction.

We further assess the scale offsets (or errors) associated with measurements made at differing scales by examining the difference in the average $\Delta \bar{T}_{s-a}$ at each scale and by condition and/or surface type, which are depicted by the horizontal solid lines in Fig. 5. The scale offsets of the 1 cm as compared to either 6.8 m or 1 km scale observations are calculated by taking the difference of the lines representing the $\Delta \bar{T}_{s-a}$ values (select offsets are presented in Table 4). When considering the full playground equipment in the sun, the mean $\Delta \bar{T}_{s-a}$ sun is 19.6 °C (horizontal orange line) at the touch-scale, while the 1 km sun value $\Delta \bar{T}_{s-a}$ mean is 8.7 °C (horizontal magenta line), giving an offset between the two of 10.8 °C. For all sun exposed surfaces, $\Delta \bar{T}_{s-a}$ of 16.0 °C is found, yet if we were to consider only the overall 6.8 m playground $\Delta \bar{T}_{s-a}$ (8.7 °C) or neighborhood $\Delta \bar{T}_{s-a}$ (12.2 °C), we would underestimate the T_s found at

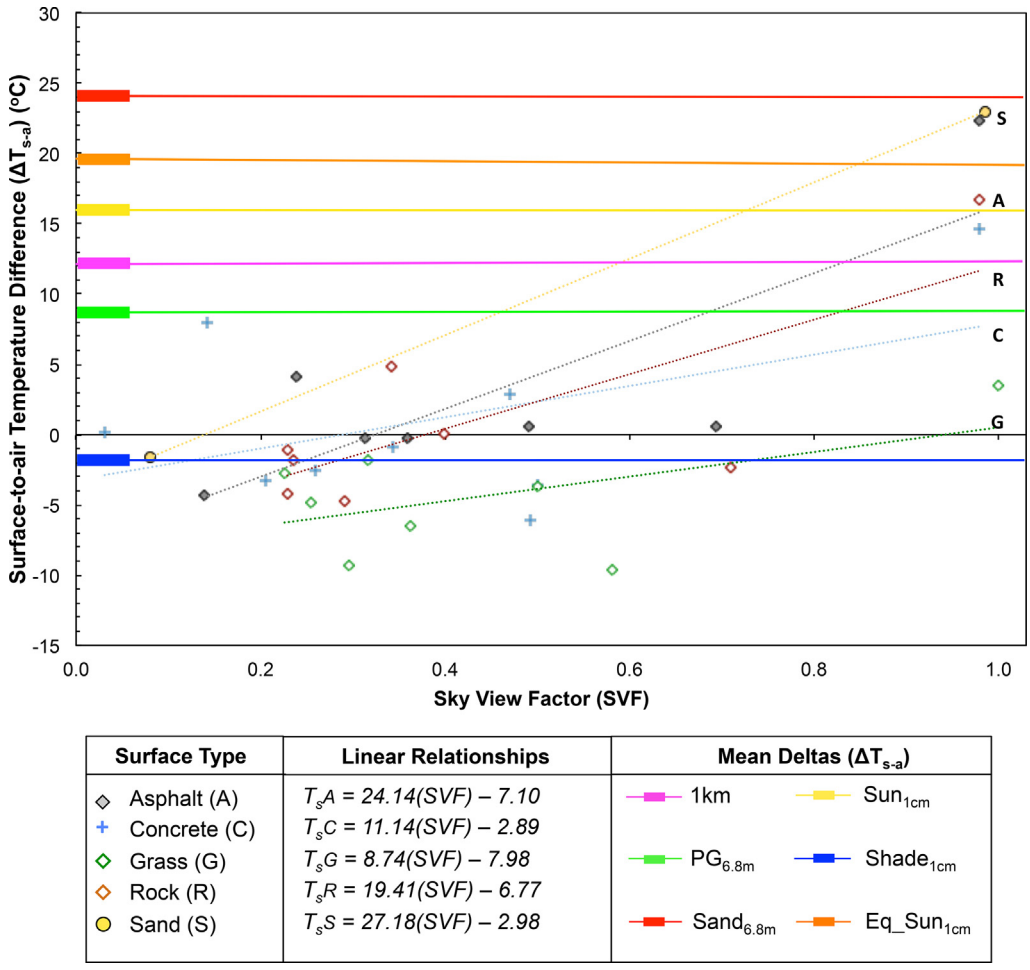

Fig. 5. Variation in mean surface-to-air temperature deltas ($\Delta\bar{T}_{s-a}$) at the 1 cm touch-scale due to change in sky view factor (SVF) for each surface type (asphalt, concrete, grass, rock, sand). Sloped regression lines represent linear relationship of ΔT_{s-a} with SVF for each surface type, with regression equations shown. Solid horizontal lines represent the $\Delta\bar{T}_{s-a}$ at various scales and surfaces: 1 km (neighborhood), $PG_{6.8m}$ (playground $\bar{T}_s$ at 6.8 m scale), $Sand_{6.8m}$ ($\bar{T}_s$ of sand at 6.8 m scale), Sun_{1cm} ($\bar{T}_s$ in sun at 1 cm scale), $Shade_{1cm}$ ($\bar{T}_s$ in shade at 1 cm scale), Eq_Sun_{1cm} ($\bar{T}_s$ of PG equipment in sun at 1 cm scale). Scale offsets (presented in Table 4) are calculated from differences in the horizontal lines compared to $\Delta\bar{T}_{s-a}$ at the 1 cm scale.

the touch-scale measurements within the playgrounds. Therefore, for all playground surfaces, there is an average *offset* of −3.8 °C if using the 6.8 m scale, and −7.3 °C using the 1 km scale, both representing a scale measurement error of underestimations in actual T_s measured at the 1 cm scale. These underestimations increase when examining playground equipment (Table 4), with offsets of −6.6 °C at the 6.8 m scale, and −10.1 °C at the 1 km scale as compared to the 1 cm scale. Hence, the coarser scales underestimate high T_s and ΔT_{s-a} found in the playgrounds.

Comparisons of the distributions of the touch-scale T_s with the overall neighborhood distribution of 6.8 m T_s (smoothed linear histogram as in Fig. 4b) are presented in Fig. 6. The handheld-IRT touch-scale T_s data, including playground equipment temperatures (Table 2), are presented as sun exposed (plot A), and in shade (plot B) for nine surface types (both ground and equipment surfaces). The sun exposed surfaces display a T_s of 54.8 °C (vertical solid gray line, plot A), while the mean in the shade for all surfaces is 38.4 °C (vertical solid black line, plot C). This 54.8 °C touch-scale sun value is 9.5 °C above the remotely sensed playground T_s of 45.3 °C (dashed turquoise line, plot C) at the 6.8 m scale, and 6.0 °C above the $\bar{T}_s$ of the full neighborhood (48.8 °C; vertical solid green line). Furthermore, select touch-scale temperature values recorded in the sun (rubber and some plastic surfaces) are outside of the range of the distribution of the 6.8 m MASTER data, as seen by comparing T_s data points in panel A to the distribution curve in panel C in Fig. 6. This again displays the inability of coarse resolution observations to discern touch-scale T_s.

These scale discrepancies clearly demonstrate that the hottest touch-scale temperatures (exceeding the material-specific thresholds; Table 1) cannot be resolved with the 6.8 m MASTER data. For example, when examining temperature pixels in the circular South playground, the remote sensing platform detects predominantly the average temperature of the sand cover (~55–60 °C) rather than the hotter equipment within these pixels, e.g., slides (63.9 and 71.7 °C), and railings (62.2–68.0 °C). Hence, remotely sensed data contains information about the mean and baseline T_s to judge the microscale distribution of T_s in the neighborhood, yet can have valuable use at a finer scale if an offset model is applied to estimate the touch-scale T_s using airborne remotely sensed microscale T_s. However, material-specific (e.g., for various types of playground equipment) and shade-specific offsets (e.g., by SVF or similar metric) are needed to accurately model these touch-scale variations.

4. Discussion

4.1. Playground design in hot climates

Contrasting surface temperatures are found between MASTER overflight observations (6.8 m resolution) and *in situ* infrared

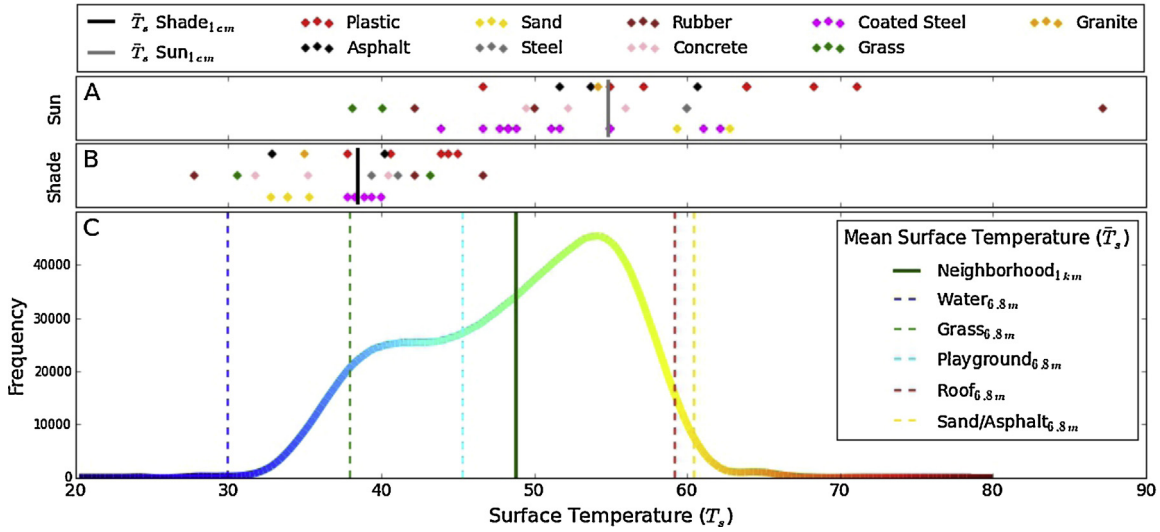

Fig. 6. Observed mean surface temperatures ($\bar{T}_s$) at the touch-scale in sun (A) and shade (B) obtained from *in situ* T_s measurements in the playgrounds, with solid vertical lines representing the 1 cm touch-scale $\bar{T}_s$ in sun and shade for the respective plot. Plot C presents the full neighborhood scale T_s smoothed distribution from Fig. 4b at the 1 km neighborhood scale from MASTER 6.8 m grid temperatures. Vertical lines in plot C represent $\bar{T}_s$ for the 1 km neighborhood scale ($\bar{T}_s$ of the 6.8 m grid temperatures), and the $\bar{T}_s$ at the 6.8 m scale for water, grass, playgrounds, roof, and sand/asphalt.

thermometer data ('touch-scale' of centimeters), where the hottest touch points of T_S found in the playgrounds are outside the distribution of the MASTER 6.8 m $\bar{T}_S$ observations and the 1 km neighborhood mean. The differences highlight the essential discrepancy that exists when working with urban $\bar{T}_S$ observations at differing scales, especially when influential material types only exist at a much finer scale on the order of centimeters. This study identifies the sub-meter "touch" scale of approximately 1 cm as the spatial scale at which surface temperatures pose a risk to children on playgrounds, and more generally of people engaged in any kind of outdoor activity in the sun. Hence, the touch-scale is the spatial scale at which data must be collected and policies of landscape design must be executed to mitigate high T_S. This is especially important in high-contact environments like playgrounds. A method to address the scale mismatch between airborne remote sensing data and touch-scale *in situ* data does not currently exist. Research in this area is at the forefront of temperature sensing technologies at fine scales, and is needed to better understand cross-scalar relationships and provide modeling capabilities to link the various scales of T_S and temperature scale offsets in conjunction with biophysical and built environmental features. The offset temperatures at each scale allow for comparisons between the average of the probability distribution of T_S at various spatial scales and/or shading conditions, for both upscaling and downscaling applications in remote sensing and climate modeling. These offset temperatures can be empirically observed for each time of day, season, material type, shading factor, and location, as the basis of improved modeling and remote sensing techniques.

Urban climate research completed in the Phoenix metropolitan area demonstrates that air and surface temperatures differ widely across area neighborhoods, with the greatest differences during summertime heat waves (e.g., Chow et al., 2012; Harlan, Brazel, Prashad, Stefanov, & Larsen, 2006; Hartz, Prashad, Hedquist, Golden, & Brazel, 2006; Jenerette, Harlan, Stefanov, & Martin, 2011; Middel et al., 2015). However, we demonstrate that *within* urban neighborhoods and small playgrounds, these surface temperatures vary significantly—and with implications for human thermal comfort and safety—at spatial scales as fine as 1 cm. Although satellite remote sensing data are more applicable for mesoscale urban climate modeling than mesoscale climate models with $\geq$ 1 km scale resolutions (e.g., Masson et al., 2003; Mishra et al., 2015), these remote sensing data are critically limited for human- and touch-scale design, missing crucial information related to touch-scale extreme T_S exposures, mean radiant temperatures, and effects of shade. These limitations are impactful especially for children, but also other people exposed to the outdoor environment during partially shaded daytime conditions, including outdoor workers and those engaged in sports or other recreational activities. However, we have demonstrated that coarser scale satellite remote sensing data does provide valuable information serving as a basis for estimating the fine-scale distribution around the average surface temperature, $\bar{T}_S$, when accompanied by an offset model to estimate the touch-scale T_S.

This scale mismatch is a consequential issue because the scale of a remotely sensed observation may result in misleading conclusions at the most important scales for urban design if inter-scalar bias exists. Here, the use of 6.8 m scale T_S is biased in such a fashion, and would dramatically underestimate the touch-scale temperature if used for urban design and decision-making related to individual-scale temperature exposure. This methodological issue results in a spatial incongruence problem due to applying area-based attributes of size, shape, and spatial means (e.g., remote sensing-based) that are insufficient for point-based (human- or touch-scale) temperature exposure (Kwan, 2012). This represents a Modifiable Areal Unit Problem (MAUP) (Houston, 2014; Openshaw & Openshaw, 1984), where spatial uncertainty is influenced by the context of measurement, and is a critical concern when using research to link science and policy. The application of data from the wrong scale results in a further issue of temporal uncertainty related to the duration of time spent in certain condition, which may not be accurate given the location or areal size of a temperature observation (e.g., Kuras et al., 2015). Such spatiotemporal uncertainties may result in unsuitable decisions concerning park design and materials for use under warm and sunny conditions, or may complicate future work with higher-resolution urban climate models that require accurate microscale information to assess adaption and UHI mitigation strategies.

The cooling effect of vegetation is documented in Phoenix, where small (<20 ha), highly vegetated neighborhood parks create 'cool islands' when situated in the midst of densely urbanized areas (Chow et al., 2011; Declet-Barreto, Brazel, Martin, Chow, & Harlan, 2013; Jenerette et al., 2007; Middel, Häb, Brazel, Martin,

& Guhathakurta, 2014). Vegetation is also found more effective at cooling hotter neighborhoods (Jenerette et al., 2015). However, this cooling effect as studied costs a substantial amount of water to achieve—an expensive proposition in a desert city. Further bioclimatic design in hot and sunny climates must employ shade as a means of effectively reducing the mean radiant temperature imposed on a human at the hottest time of the day, and thus overall heat stress (Ali-Toudert & Mayer, 2007; Matzarakis & Endler, 2010; Shashua-Bar, Pearlmutter, & Erell, 2011). We show that shade generates a T_s that is similar or lower than the reference temperature, T_a, reversing the general trend where $T_s > T_a$. Although the T_{mrt} is reduced by the shade sail—which effectively reduces experienced temperature—the comparisons to T_a reductions within related studies in Phoenix and other cities from vegetation is only valid when examining results under the shade of trees, as there is no evaporative cooling effect from vegetation under the shade sail. However, this study concurs with studies finding T_s reduction from many types of shade (e.g., Antoniadis, Katsoulas, Papanastasiou, Christidou, & Kittas, 2015; Ketterer & Matzarakis, 2014b; Lin & Lin, 2010), where all shade, whether tree or artificial (e.g., mesh or shade sails), is found effective in reducing the T_s in the hot and arid climate to safe levels. This would in turn reduce thermal discomfort from sensible heat fluxes as found in related shade studies (e.g., Antoniadis et al., 2015; Shashua-Bar et al., 2011). Further microclimate factors influencing heat stress and thermal discomfort—in addition to exchanges of solar radiation and sensible heat (via convection) discussed here—include evaporation and longwave emittance (Kenny, Warland, Brown, & Gillespie, 2009; Vanos, Warland, Kenny, & Gillespie, 2010), with metabolic activity increasing core and skin temperatures due to increased heat generation (Vanos, Warland, Gillespie, & Kenny, 2012; Yao, Lian, Liu, & Shen, 2007).

A study examining the energy budgets and/or the air cooling potential of the differing types of shade can provide valuable information within a hot, arid city that can address the co-benefits of water use for vegetation and evaporative cooling versus the cost for water use at different times of the year. The effect of shade on T_s is comparable to the effect of moistening a surface with water, and shade can be utilized over any surface or urban space, not just vegetated surfaces and specially designed water features. Artificial shade is a very effective and flexible means of reducing T_s and T_{mrt}, and of improving thermal comfort and thermal safety in spaces used by people during a specific time of day, without the need for water use. This shade should employ sound design principles to target the locations, times of day, and times of year when people will be using a specific space while it is too hot; the optimal type of shade might be different for a bus stop as compared with a playground. In Phoenix and similar cities, shade should be provided for all playgrounds during the warmer seasons to avoid unsafe touch-scale T_s. As an added benefit for air conditioned buildings, shade on exterior building walls will reduce wall T_s, and shade on windows will reduce shortwave radiative loading, both reducing energy costs of air conditioning. Our findings and data also speak directly to such building energy considerations. In a very hot climate like Phoenix, carefully designed shade has the helpful characteristic of lowering thermal loads and T_s during the daytime year-round, where daytime reductions in T_s may be more effective in reducing health risks than nighttime (Jenerette et al., 2015). In a colder climate, it might be important to avoid shading the microenvironment during the day during winter. Our findings and design recommendations should be interpreted accordingly, and further research conducted in those other urban geographies and seasonalities.

The state of Arizona leads the U.S. in both deaths from heat exposure (Centers for Disease Control and Prevention, 2006) and extreme heat events representative of severe outdoor thermal risks to urban dwellers (Grossman-Clarke, Zehnder, Loridan, & Grimmond, 2010). The Phoenix metropolitan area is among the hottest urban regions in the world, with heat amplified by one of the strongest UHIs worldwide (Chow et al., 2012). The Town of Gilbert and the neighborhood of Power Ranch possess an upper socio-economic demographic with modern parks such as the study site playgrounds that are subject to advanced planning and safety standards. Therefore this neighborhood is typical of the global extreme both in terms of a hot urban climate and of recent best practices of neighborhood adaptation to urban climate, including relatively safe playground materials and the use of targeted shade. The findings of this study are even more important in communities that do not yet follow modern playground safety standards. Results from this extreme circumstance will therefore be increasingly relevant globally and in the future as outdoor urban environments warm and planning practices modernize.

4.2. Health and safety standards in playgrounds related to temperature

Urban-dwelling children are routinely identified as a vulnerable population in environmental health review literature related to heat-health and climate change (e.g., Ebi & Paulson, 2010; English et al., 2009; Perera, 2008). The current findings and ensuing discussion provide important avenues for mitigating heat and burn exposures to children and the associated negative health consequences in playgrounds, as well as mechanisms for adapting the urban environment to manage increasing temperatures and population growth. Although many days in Phoenix now and in the future exhibit extreme surface and air temperatures, shade cover can result in a wider temporal window within which a child can safely play without the risk of being burned by a surface.

The CPSC works with ASTM International (ASTM) (formerly American Society for Testing and Materials) to ensure playground safety via equipment standards. The current standard in use is the ASTM F1487-Standard Consumer Safety Performance Specification for Playground Equipment for Public Use (ASTM F1487, 2011). Although its main purpose is to reduce life-threatening and debilitating injuries, many of the standards are employed voluntarily rather than mandated, which can result in vague and inadequate procedures for playground safety. In general, few if any mandatory standards exist for surface temperature modification or reduction, although guidelines are available. The full outline and processes for creating mandatory rules and guidelines are outlined in Earls (2011) and Ford et al. (2011). Ford et al. (2011) reported results from the In-Depth-Injury Reports (IDIs) issued by the CSPC[1] (O'Brien, 2009) revealing 14 severe burns in children occurring on various playground surfaces (2001–2008), with nine being 2nd or 3rd degree burns.

Materials with high heat capacities and/or thermal conductivities (e.g., black rubber, concrete, asphalt, artificial turf, steel, aluminum) transfer heat quickly to the skin, and thus have a higher potential to cause extensive burns. Results here show that in direct sunlight, many of these materials can reach temperatures that are above the thresholds for burn injury to a child (CPSC, 2010; Ford et al., 2011; ISO 13732, 2010). O'Brien (2009) reported playground slides to be the second most common equipment for burns (after walking surfaces), with slides contributing to 29% of cases report by the IDIs from 2001 to 2008. Although safer than metal, the plastic slides in the study parks reached $\bar{T}_s$ of 67.8 °C in direct sunlight.

[1] IDIs are part of the National Electronic Injury Surveillance System (NEISS) that is run by CPSC to report injuries in the US (http://www.cpsc.gov/en/Research–Statistics/NEISS-Injury-Data/).

Walking and standing surfaces made of rubber, concrete, asphalt, and metal exposed to the sun were also found to reach temperatures approaching or above burn threshold temperatures (see Tables 1 and 2), thus increasing the likelihood of burns to the feet which can occur when children are playing and easily remove/lose footwear and run or fall onto a scalding surface (e.g., O'Brien, 2009). Based on CPSC reported data from 2001 to 2011, Ford et al. (2011) reported 21 of 38 burn cases occurring on walking surfaces, including rubber mats, concrete, and asphalt. The application of various shock-absorbing ground materials (sand, wood chips, pea gravel, rubber) in playgrounds is based on reducing the risk of injury due to falling (CPSC, 2010), yet these surfaces commonly reach the highest T_s in the sun. However, if these surfaces are already in place or have a mandatory use, then our results show that providing shade cover in *any* form can reduce T_s to a safe level. Shade on "walking" type materials that cover large areas occupied by people will also mitigate T_{mrt} in that space, providing a substantial thermal comfort benefit that extends beyond reduction in the risk of burns.

Although greater attention has been given to other causes of serious playground injuries in equipment design (Branson et al., 2012; Mack, Hudson, & Thompson, 1997; Spiegal, Gill, Harbottle, & Ball, 2014), the likely underreporting of heat-related injuries in children (e.g., Yeo, 2004) and lack of mandatory rules warrant greater attention to the issue. According to the ASTM, further analyses similar to ASTM C1057 (2012) is required using a thermesthesiometer, an instrument specific for burn hazard measurement (Marzetta, 1974; Ungar & Stroud, 2010), or employing a mathematical model. This paper's methods are the beginning of such a mathematical model. The urban design community should carefully consider whether evidence-based touch-scale temperature and shade standards should be adopted for playgrounds and other spaces occupied by people during hot daytime hours. Based on results of this study, we recommend that the adoption of new standards be considered.

Playgrounds serve the purpose of eliciting physical activity, while providing spaces that are safe, thermally comfortable, functional, accessible, and healthy. These services are of paramount importance in maintaining child health and well-being (Ciucci et al., 2013; Fjørtoft, 2004; Wolch et al., 2011). The solution to reducing playground heat illness and surface burns on extreme heat days is not to prohibit play, but to encourage safe play, invoke awareness, and/or limit play to the morning or evening hours. Quality play settings result in increased activity and improved health (e.g., lessen obesity and diabetes) (Barnes, 2011) and social networking (Bessesen, 2008; Sallis, Floyd, Rodríguez, & Saelens, 2012; Wolch et al., 2011), increased cognitive and motor development (Boldemann et al., 2006; Brussoni, Olsen, Pike, & Sleet, 2012; Ciucci et al., 2011, 2013; Wenner, 2009), and improved behavior (Bessesen, 2008; Ciucci et al., 2013; Lagacé-Séguin & d'Entremont, 2005) and learning (Taylor & Kuo, 2009). Quantifying both the $\Delta\bar{T}_{s-a}$ over various surfaces and the scale offsets of these deltas can produce accurate and vital information for reducing playground T_s through bioclimatic design. Such evidence-based design is applicable for public health agencies or local community organizations and warranted in order to achieve thermally safe playgrounds during the warm season and/or in warm climates.

4.3. Future work

This is a foundational study supporting an increased effort to create viable methods for applying remotely sensed data at finer environmental scales in order to advance public health and urban design practice (e.g., White-Newsome et al., 2013). Promising future opportunities exist in this research domain to generate more evidence-based research largely centered on child-specific physiological responses and behavior in order to optimally incorporate effective bioclimatic design in outdoor playgrounds (e.g., mandating a certain amount of shade cover conserved/implemented in schoolyards). Findings from this study lay the groundwork for future research to explore the systematic relationships between *in situ* touch-scale surface temperatures, remotely sensed microscale T_s, and those represented by urban climate models. Future work is needed to develop a robust empirical mathematical model of scale offsets in $\Delta\bar{T}_{s-a}$ to link remotely sensed data at a given scale (e.g., 6.8 m) with 1 cm touch scale surface temperature data based on material, color, and biophysical data (i.e., solar angle, transmissivity, microclimate, shade type, etc.), and to extend this database and modeling work to other times of day, seasons, locations, and climates. This will provide vital information to the ASTM, CPSC, and urban landscape architects to make decisions at the correct scale.

4.4. Conclusions

We presented surface temperature data at multiple scales within two playgrounds during hot, dry weather conditions in Gilbert, AZ. High surface temperatures of playground equipment and ground surfaces exposed to the sun were routinely found from the *in situ* touch-scale (1 cm) measurements, which were not detected by the airborne MASTER sensor (6.8 m resolution). Select touch-scale temperatures approached or surpassed thresholds of burn temperatures to children. Temperature deltas representing surface-to-air differences were highest for playground equipment and ground surface touch-scale measurements in sun ($\Delta\bar{T}_{s-a}$ = 19.6 and 15.9 °C, respectively). Scale offsets (errors due to the scale of measurement) systematically underestimated the T_s and ΔT_{s-a} when using micro-scale and neighborhood scale T_s data rather than touch-scale. This T_s underestimation error at the coarser scales can cause spatial uncertainty in linking urban climate research to policy, yet may be valuable for use at a finer scale if an offset model is applied to account for this error.

Shade from both natural (tree) and artificial (shade sail) sources—no matter the type—reduced touch-scale playground T_s to safe levels, with a $\Delta\bar{T}_{s-a}$ of–24.3 °C in the shade as compared to the sun for all surfaces. The relatively new installation of the large shade sail in the North Playground of Power Ranch demonstrates the effectiveness of shade at reducing the potential for burns, providing empirical evidence that in hot climates or during warm seasons, the temporal window within which a child may be burned on a surface is completely diminished through the use of shade. This is a reduction not detected by the overhead-angle of airborne remotely sensed data. Thus, coarser scale data or models (such as urban climate models) cannot resolve T_s at the proper scale for playground design. This discrepancy can lead to inaccuracies in decision-making and applications related to health-outcome analysis, establishment of playground safety burn standards (reduce risk of heat illness and injuries), urban park design guidelines and policies, and urban cooling adaptation strategies and UHI mitigation. Finally, our results strongly motivate new touch-scale urban temperature research, and the provision that bioclimatic principles and effective green space should have a central position in landscape architecture, urban sustainability, and urban planning policy for outdoor environments, particularly parks and children's play places.

Acknowledgements

The authors would like to acknowledge the Power Ranch Community Association's (PRCA) support of the data collection and David Hondula of ASU for aid in manuscript review and insightful discussions. The collection of the MASTER data was jointly funded by the NSF grants GEO-0816168, BCS-1026865. Work was also

funded by the NSF grant EF-1049251, and a grant to Arizona State University by the Salt River Project. Any opinions, findings, and conclusions or recommendations expressed in this material are those of the author(s) and do not necessarily reflect those of the National Science Foundation. Benjamin Ruddell discloses membership on the Board of Directors of the PRCA, which proposed construction of shade structures at neighborhood playgrounds.

Appendix A. Supplementary data

Supplementary data associated with this article can be found, in the online version, at http://dx.doi.org/10.1016/j.landurbplan.2015.10.007.

References

Adachi, S. A., Hara, M., Takahashi, H. G., Ma, X., Yoshikane, T., & Kimura, F. (2013). *Changes in urban climate due to future land-use changes based on population changes in the Nagoya region*. pp. 455. *AGU fall meeting abstracts* (Vol. 1)

Ali-Toudert, F., & Mayer, H. (2007). Effects of asymmetry, galleries, overhanging facades and vegetation on thermal comfort in urban street canyons. *Solar Energy*, *81*(6), 742–754.

Antoniadis, D., Katsoulas, N., Papanastasiou, D., Christidou, V., & Kittas, C. (2015). Evaluation of thermal perception in schoolyards under Mediterranean climate conditions. *International Journal of Biometeorology*, 1–16.

ASTM 1055. (2014). *Standard guide for heated system surface conditions that produce contact burn injuries*. West Conshohocken, PA. http://www.astm.org/Standards/C1055.htm

ASTM C1057. (2012). *Standard practice for determination of skin contact temperature from heated surfaces using a mathematical model and thermesthesiometer*. West Conshohocken, PA. http://dx.doi.org/10.1520/C1057

ASTM F1487. (2011). *Standard consumer safety performance specification for playground equipment for public use. No. F1487-07ae1*. West Conshohocken, PA. http://dx.doi.org/10.1520/F1487-11

Balbus, J. M., & Malina, C. (2009). Identifying vulnerable subpopulations for climate change health effects in the United States. *Journal of Occupational and Environmental Medicine*, *51*(1), 33–37.

Barnes, M. (2011). *White house task force on childhood obesity report to the president: One year progress report*. Washington, DC. http://www.letsmove.gov/sites/letsmove.gov/files/Obesity_update_report.pdf

Bessesen, D. H. (2008). Update on obesity. *Journal of Clinical Endocrinology & Metabolism*, *93*(6), 2027–2034.

Board on Atmospheric Sciences and Climate (BASC) Summer Community Workshop. (2012). *Urban meteorology: Forecasting, monitoring, and meeting users' needs* (15th ed.). Washington, DC: National Research Council (U.S.), The National Academies Press. http://www.nap.edu/openbook.php?record_id=13328

Boldemann, C., Blennow, M., Dal, H., Mårtensson, F., Raustorp, A., Yuen, K., et al. (2006). Impact of preschool environment upon children's physical activity and sun exposure. *Preventive Medicine*, *42*(4), 301–308.

Branson, L. J., Latter, J., Currie, G. R., Nettel-Aguirre, A., Embree, T., & Hagel, B. E. (2012). The effect of surface and season on playground injury rates. *Paediatrics & Child Health*, *17*(9), 485.

Brown, R. D., Vanos, J. K., Kenny, N. A., & Lenzholzer, S. (2015). Designing urban parks that ameliorate the effects of climate change. *Landscape and Urban Planning*, http://dx.doi.org/10.1016/j.landurbplan.2015.02.006

Brussoni, M., Olsen, L. L., Pike, I., & Sleet, D. A. (2012). Risky play and children's safety: Balancing priorities for optimal child development. *International Journal of Environmental Research and Public Health*, *9*(9), 3134–3148.

Campbell, G. S., & Norman, J. M. (1998). *An introduction to environmental biophysics* (2nd ed.). New York: Springer.

Centers for Disease Control and Prevention. (2006). Heat-related deaths—United States, 1999–2003. *Morbidity and Mortality Weekly Report*, *55*, 796–798.

Cheng, X., Wei, B., Chen, G., Li, J., & Song, C. (2014). Influence of park size and its surrounding urban landscape patterns on the park cooling effect. *Journal of Urban Planning and Development*, http://dx.doi.org/10.1061/(ASCE)UP.1943-5444.0000256

Chow, W. T. L., Brennan, D., & Brazel, A. J. (2012). Urban heat island research in Phoenix, Arizona: Theoretical contributions and policy applications. *Bulletin of the American Meteorological Society*, *93*(4), 517–530.

Chow, W. T. L., Pope, R. L., Martin, C. A., & Brazel, A. J. (2011). Observing and modeling the nocturnal park cool island of an arid city: Horizontal and vertical impacts. *Theoretical and Applied Climatology*, *103*(1–2), 197–211.

Ciucci, E., Calussi, P., Menesini, E., Mattei, A., Petralli, M., & Orlandini, S. (2011). Weather daily variation in winter and its effect on behavior and affective states in day-care children. *International Journal of Biometeorology*, *55*(3), 327–337.

Ciucci, E., Calussi, P., Menesini, E., Mattei, A., Petralli, M., & Orlandini, S. (2013). Seasonal variation, weather and behavior in day-care children: A multilevel approach. *International Journal of Biometeorology*, *57*(6), 845–856.

CPSC. (2010). *Handbook for public playground safety*. Bethesda, MD. http://www.cpsc.gov/PageFiles/122149/325.pdf

Declet-Barreto, J., Brazel, A. J., Martin, C. A., Chow, W. T. L., & Harlan, S. L. (2013). Creating the park cool island in an inner-city neighborhood: Heat mitigation strategy for Phoenix, AZ. *Urban Ecosystems*, *16*(3), 617–635.

Earls, A. (2011). The CPSC-ASTM collaboration. *ASTM Standardization News*, *39*(1), 32–35.

Ebi, K. L., & Paulson, J. A. (2010). Climate change and child health in the United States. *Current Problems in Pediatric and Adolescent Health Care*, *40*(1), 2–18.

English, P. B., Sinclair, A. H., Ross, Z., Anderson, H., Boothe, V., Davis, C., et al. (2009). Environmental health indicators of climate change for the United States: Findings from the State Environmental Health Indicator Collaborative. *Environmental Health Perspectives*, *117*(11), 1673–1681.

Environmental Protection Agency. (2014). *Cooling summertime temperatures.*. http://www.epa.gov/heatislands/resources/pdf/HIRIbrochure.pdf

Erell, E., Pearlmutter, D., & Williamson, T. (2012). *Urban microclimate: Designing the spaces between buildings*. Routledge.

Falk, B., & Dotan, R. (2008). Children's thermoregulation during exercise in the heat – A revisit. *Applied Physiology, Nutrition, and Metabolism*, *33*(2), 420–427.

Fjørtoft, I. (2004). Landscape as playscape: The effects of natural environments on children's play and motor development. *Children Youth and Environments*, *14*(2), 21–44.

Ford, G., Moriarty, A., Riches, D., & Walker, S. (2011). *Playground equipment: Classification & burn analysis*. Bethesda, MD. http://www.wpi.edu/Pubs/E-project/Available/E-project-122111-202154/unrestricted/WPI_Final_Report_IQP-CPSC.pdf

Grossman-Clarke, S., Zehnder, J. A., Loridan, T., & Grimmond, C. S. B. (2010). Contribution of land use changes to near-surface air temperatures during recent summer extreme heat events in the Phoenix metropolitan area. *Journal of Applied Meteorology and Climatology*, *49*(8), 1649–1664.

Harlan, S. L., Brazel, A. J., Prashad, L., Stefanov, W. L., & Larsen, L. (2006). Neighborhood microclimates and vulnerability to heat stress. *Social Science and Medicine*, *63*(11), 2847–2863.

Harlan, S. L., Declet-Barreto, J. H., Stefanov, W. L., & Petitti, D. B. (2013). Neighborhood effects on heat deaths: Social and environmental predictors of vulnerability in Maricopa County, Arizona. *Environmental Health Perspectives*, *121*(2), 197.

Harlan, S. L., & Ruddell, D. M. (2011). Climate change and health in cities: Impacts of heat and air pollution and potential co-benefits from mitigation and adaptation. *Current Opinion in Environmental Sustainability*, *3*(3), 126–134.

Hartz, D. A., Prashad, L., Hedquist, B. C., Golden, J., & Brazel, A. J. (2006). Linking satellite images and hand-held infrared thermography to observed neighborhood climate conditions. *Remote Sensing of Environment*, *104*(2), 190–200.

Hondula, D. M., Davis, R. E., Leisten, M. J., Saha, M. V., Veazey, L. M., & Wegner, C. R. (2012). Fine-scale spatial variability of heat-related mortality in Philadelphia County, USA, from 1983–2008: A case-series analysis. *Environmental Health*, *11*(1), 1–11.

Hook, S. J., Myers, J. J., Thome, K. J., Fitzgerald, M., & Kahle, A. B. (2001). The MODIS/ASTER airborne simulator (MASTER)—A new instrument for earth science studies. *Remote Sensing of Environment*, *76*(1), 93–102.

Houston, D. (2014). Implications of the modifiable areal unit problem for assessing built environment correlates of moderate and vigorous physical activity. *Applied Geography*, *50*, 40–47.

HUSD. (2015a). *Higley United School District*. Welcome Centennial Elementary. http://www.husd.org/Page/4646

HUSD. (2015b). *Higley United School District*. Welcome, Power Ranch Elementary. http://www.husd.org/Domain/1525

ISO 13732. (2010). *ISO 13732-3: Ergonomics of the thermal environment. Methods for the assessment of human responses to contact with surfaces. Hot surfaces*. Geneva, Switzerland: Vernier.

Jenerette, G. D., Harlan, S. L., Brazel, A., Jones, N., Larsen, L., & Stefanov, W. L. (2007). Regional relationships between surface temperature, vegetation, and human settlement in a rapidly urbanizing ecosystem. *Landscape Ecology*, *22*(3), 353–365. http://dx.doi.org/10.1007/s10980-006-9032-z

Jenerette, G. D., Harlan, S. L., Buyantuev, A., Stefanov, W. L., Declet-Barreto, J., Ruddell, B. L., et al. (2015). Micro scale urban surface temperatures are related to land cover features and residential heat-related health impacts in Phoenix, AZ, USA. *Landscape Ecology*, http://dx.doi.org/10.1007/s10980-015-0284-3

Jenerette, G. D., Harlan, S. L., Stefanov, W. L., & Martin, C. A. (2011). Ecosystem services and urban heat riskscape moderation: Water, green spaces, and social inequality in Phoenix, USA. *Ecological Applications*, *21*(7), 2637–2651.

Johansson, E., Thorsson, S., Emmanuel, R., & Krüger, E. (2014). Instruments and methods in outdoor thermal comfort studies – The need for standardization. *Urban Climate*, *10*, 346–366.

Kántor, N., & Unger, J. (2011). The most problematic variable in the course of human-biometeorological comfort assessment—The mean radiant temperature. *Central European Journal of Geosciences*, *3*(1), 90–100.

Karl, T. R., Melillo, J. M., & Peterson, T. C. (2009). *Global climate change impacts in the United States*. Cambridge University Press.

Kenny, N. A., Warland, J. S., Brown, R. D., & Gillespie, T. G. (2009). Part A: Assessing the performance of the COMFA outdoor thermal comfort model on subjects performing physical activity. *International Journal of Biometeorology*, *53*(5), 415–428.

Ketterer, C., & Matzarakis, A. (2014a). Human-biometeorological assessment of heat stress reduction by replanning measures in Stuttgart, Germany. *Landscape and Urban Planning*, *122*, 78–88.

Ketterer, C., & Matzarakis, A. (2014b). Human-biometeorological assessment of the urban heat island in a city with complex topography – The case of Stuttgart, Germany. *Urban Climate*, *10*, 573–584.
Knez, I., Thorsson, S., Eliasson, I., & Lindberg, F. (2009). Psychological mechanisms in outdoor place and weather assessment: Towards a conceptual model. *International Journal of Biometeorology*, *53*(1), 101–111.
Koppe, C., & Jendritzky, G. (2005). Inclusion of short-term adaptation to thermal stresses in a heat load warning procedure. *Meteorologische Zeitschrift*, *14*(2), 271–278.
Krayenhoff, E. S., & Voogt, J. A. (2007). A microscale three-dimensional urban energy balance model for studying surface temperatures. *Boundary-Layer Meteorology*, *123*(3), 433–461.
Kuras, E. R., Hondula, D. M., & Brown-Saracino, J. (2015). Heterogeneity in individually experienced temperatures (IETs) within an urban neighborhood: Insights from a new approach to measuring heat exposure. *International Journal of Biometeorology*, 1–10.
Kwan, M.-P. (2012). The uncertain geographic context problem. *Annals of the Association of American Geographers*, *102*(5), 958–968.
Lagacé-Séguin, D. G., & d'Entremont, M. L. (2005). Weathering the preschool environment: Affect moderates the relations between meteorology and preschool behaviors. *Early Child Development and Care*, *175*(5), 379–394.
Lin, B.-S., & Lin, Y.-J. (2010). Cooling effect of shade trees with different characteristics in a subtropical urban park. *HortScience*, *45*(1), 83–86.
Luber, G., Knowlton, K., Balbus, J., Frumkin, H., Hayden, M., Hess, J., et al. (2014). Human health. In G. W. Melillo, J. M. Richmond, & T. C. Yohe (Eds.), *U.S. Global Change Research Program* (pp. 220–256). http://dx.doi.org/10.7930/J0PN93H5
Mack, M. G., Hudson, S., & Thompson, D. (1997). A descriptive analysis of children's playground injuries in the United States 1990–4. *Injury Prevention*, *3*(2), 100–103.
Marzetta, L. A. (1974). *Engineering and construction manual for an instrument to make burn hazard measurements in consumer products*. Washington, DC.
Masson, V., Champeaux, J.-L., Chauvin, F., Meriguet, C., & Lacaze, R. (2003). A global database of land surface parameters at 1-km resolution in meteorological and climate models. *Journal of Climate*, *16*(9), 1261–1282.
Masson, V., Marchadier, C., Adolphe, L., Aguejdad, R., Avner, P., Bonhomme, M., et al. (2014). Adapting cities to climate change: A systemic modelling approach. *Urban Climate*, *10*, 407–429.
Matzarakis, A., & Endler, C. (2010). Climate change and thermal bioclimate in cities: Impacts and options for adaptation in Freiburg, Germany. *International Journal of Biometeorology*, *54*(4), 479–483.
Matzarakis, A., Rutz, F., & Mayer, H. (2010). Modelling radiation fluxes in simple and complex environments: Basics of the RayMan model. *International Journal of Biometeorology*, *54*(2), 131–139.
Mayer, H., & Höppe, P. (1987). Thermal comfort of man in different urban environments. *Theoretical and Applied Climatology*, *38*, 43–49.
McCarthy, M. P., & Sanderson, M. G. (2011). Urban heat islands: Sensitivity of urban temperatures to climate change and heat release in four European Cities. *Cities and Climate Change*, 175.
McGeehin, M. A., & Mirabelli, M. (2001). The potential impacts of climate variability and change on temperature-related morbidity and mortality in the United States. *Environmental Health Perspectives*, *109*(Suppl 2), 185–189.
Meehl, G. A., & Tebaldi, C. (2004). More intense, more frequent, and longer lasting heat waves in the 21st century. *Science*, *305*(5686), 994–997.
Metje, N., Sterling, M., & Baker, C. J. (2008). Pedestrian comfort using clothing values and body temperatures. *Journal of Wind Engineering & Industrial Aerodynamics*, *96*(4), 412–435.
Middel, A., Chhetri, N., & Quay, R. (2015). Urban forestry and cool roofs: Assessment of heat mitigation strategies in Phoenix residential neighborhoods. *Urban Forestry & Urban Greening*, *14*(1), 178–186.
Middel, A., Häb, K., Brazel, A. J., Martin, C. A., & Guhathakurta, S. (2014). Impact of urban form and design on mid-afternoon microclimate in Phoenix Local Climate Zones. *Landscape and Urban Planning*, *122*, 16–28.
Mishra, V., Ganguly, A. R., Nijssen, B., & Lettenmaier, D. P. (2015). Changes in observed climate extremes in global urban areas. *Environmental Research Letters*, *10*(2), 24005.
Moogk-Soulis, C. (2010). Schoolyard heat islands: A case in Waterloo, Ontario. In *5th Canadian urban forest conference* (pp. 24–27).
Moore, R., & Cosco, N. (2014). Growing up green: Naturalization as a health promotion strategy in early childhood outdoor learning environments. *Children Youth and Environments*, *24*(2), 168–191.
National Oceanic and Atmospheric Administration. (2012). *Comparative climatic data for the United States through 2012*. Asheville, NC. http://www1.ncdc.noaa.gov/pub/data/ccd-data/CCD-2012.pdf#sthash.UpnVUfyR.dpuf
O'Brien, C. (2009). *Injuries and investigated deaths associated with playground equipment, 2001–2008*. Bethesda, MD. http://www.cpsc.gov/library/foia/foia10/os/playground.pdf
Oke, T. R. (1988). The urban energy balance. *Progress in Physical Geography*, *12*, 471.
Oliveria, S. A., Saraiya, M., Geller, A. C., Heneghan, M. K., & Jorgensen, C. (2006). Sun exposure and risk of melanoma. *Archives of Disease in Childhood*, *91*(2), 131–138.
Openshaw, S., & Openshaw, S. (1984). The modifiable areal unit problem. In *Geo Abstracts University of East Anglia*.
Parsons, K. C. (2003). *Human Thermal Environments: The effects of hot, moderate and cold environments on human health, comfort and performance* (2nd ed.). New York, NY: Taylor and Francis.
Paul, K. C., Pal, A. K., Ghosh, A. K., & Chakraborty, N. R. (2004). Thermal measurements of coating films used for surface insulation and protection. *Surface Coatings International Part B: Coatings Transactions*, *87*(2), 137–141.
Perera, F. P. (2008). Children are likely to suffer most from our fossil fuel addiction. *Environmental Health Perspectives*, *116*(8), 987–990.
Petitti, D., Hondula, D. M., Yang, S., Harlan, S. L., & Chowell, G. (2015). Multiple trigger points for quantifying heat-health impacts: New evidence from a hot climate. *Environmental Health Perspectives*, http://dx.doi.org/10.1289/ehp.1409119
Sallis, J. F., Floyd, M. F., Rodríguez, D. A., & Saelens, B. E. (2012). Role of built environments in physical activity, obesity, and cardiovascular disease. *Circulation*, *125*(5), 729–737.
Shashua-Bar, L., Pearlmutter, D., & Erell, E. (2011). The influence of trees and grass on outdoor thermal comfort in a hot-arid environment. *International Journal of Climatology*, *31*(10), 1498–1506.
Sheridan, S. C. (2002). The redevelopment of a weather-type classification scheme for North America. *International Journal of Climatology*, *22*(1), 51–68.
Sheridan, S. C. (2015). *Synoptic scale classification*.. http://sheridan.geog.kent.edu/ssc.html
Spiegal, B., Gill, T. R., Harbottle, H., & Ball, D. J. (2014). Children's play space and safety management rethinking the role of play equipment standards. *SAGE Open*, *4*(1), 2158244014522075.
Stefanov, W. L., Prashad, L., Eisinger, C., Brazel, A., & Harlan, S. L. (2004). Investigation of human modifications of landscape and climate in the Phoenix Arizona Metropolitan area using MASTER data. *Pan*, *2*, 2–8.
Strong, D., Tahir, A., & Verma, S. (2007). Not fun in the sun: Playground safety in a heatwave. *Emergency Medicine Journal*, *24*(9), 2. http://dx.doi.org/10.1136/emj.2006.041657
Taylor, A. F., & Kuo, F. E. (2009). Children with attention deficits concentrate better after walk in the park. *Journal of Attention Disorders*, *12*(5), 402–409.
Tebaldi, C., Hayhoe, K., Arblaster, J. M., & Meehl, G. A. (2006). Going to the extremes: An intercomparison of model-simulated historical and future changes in extreme events. *Climatic Change*, *79*, 185–211.
Thorsson, S., Honjo, T., Lindberg, F., Eliasson, I., & Lim, E.-M. (2007). Thermal comfort and outdoor activity in Japanese urban public places. *Environment and Behavior*, *39*(5), 660–684.
U.S. Census Bureau. (2015). *2009–2013 5-year American Community Survey*. U.S. Bureau of the Census. http://www.census.gov/acs/www/
Ungar, E., & Stroud, K. (2010). A new approach to defining human touch temperature standards. In *40th International conference on environmental systems* Barcelona, Spain.
Van Der Meer, F., & de Jong, S. M. (2001). . *Imaging spectrometry: Basic principles and prospective applications* (Vol. 1) Springer Science & Business Media.
Vanos, J. (2015). Children's health and vulnerability in outdoor microclimates: A comprehensive review. *Environment International*, *76*, 1–15.
Vanos, J. K., Warland, J. S., Gillespie, T. J., Slater, G. A., Brown, R. D., & Kenny, N. A. (2012). Human energy budget modeling in urban parks in Toronto, ON and applications to emergency heat stress preparedness. *Journal of Applied Meteorology & Climatology*, *51*(9), 1639–1653.
Vanos, J. K., Warland, J. S., Kenny, N. A., & Gillespie, T. J. (2010). Review of the physiology of human thermal comfort while exercising in urban landscapes and implications for bioclimatic design. *International Journal of Biometeorology*, *54*(4), 319–334.
Vanos, J., Warland, J., Gillespie, T., & Kenny, N. (2012). Thermal comfort modelling of body temperature and psychological variations of a human exercising in an outdoor environment. *International Journal of Biometeorology*, *56*(1), 21–32.
Walsh, J., Wuebbles, D., Hayhoe, K., Kossin, J., Kunkel, K., Stephens, G., et al. (2014). Climate change impacts in the United States. In J. M. Melillo, T. C. Richmond, & G. W. Yohe (Eds.), *The third national climate assessment* (pp. 19–67). US Global Change Research Program.
Wenger. (2003). The regulation of body temperature. In G. Rhoades, & R. Tanner (Eds.), *Medical physiology* (2nd ed., Vol. 1, pp. 527–550). Boston: Little Brown.
Wenner, M. (2009). *The serious need for play*. Scientific America. http://www.scientificamerican.com/article/the-serious-need-for-play/
White-Newsome, J. L., Brines, S. J., Brown, D. G., Dvonch, J. T., Gronlund, C. J., Zhang, K., et al. (2013). Validating satellite-derived land surface temperature with in situ measurements: A public health perspective. *Environmental Health Perspectives*, *121*(8), 925.
Wolch, J., Jerrett, M., Reynolds, K., McConnell, R., Chang, R., Dahmann, N., et al. (2011). Childhood obesity and proximity to urban parks and recreational resources: A longitudinal cohort study. *Health & Place*, *17*(1), 207–214.
Yaghoobian, N., Kleissl, J., & Krayenhoff, E. S. (2010). Modeling the thermal effects of artificial turf on the urban environment. *Journal of Applied Meteorology and Climatology*, *49*(3), 332–345.
Yao, Y., Lian, Z., Liu, W., & Shen, Q. (2007). Experimental study on skin temperature and thermal comfort of the human body in a recumbent posture under uniform thermal environments. *Indoor and Built Environment*, *16*(6), 505.
Yeo, T. P. (2004). Heat stroke: A comprehensive review. *ACN Clinical Issues: Advanced Practice in Acute and Critical Care*, *2*, 280–293.